Interaction of the Beryllium Cation with the Molecular Hydrogen and Deuterium

Denis G. Artiukhin,[†] Jacek Kłos,[‡] Evan J. Bieske,[¶] and Alexei A. Buchachenko[*,†]

Department of Chemistry, Moscow State University, Moscow 119991, Russia, Department of Chemistry and Biochemistry, University of Maryland, College Park, Maryland, 20742-2021, USA, and School of Chemistry, The University of Melbourne, Parkville, VIC 3010, Australia

E-mail: alexei@classic.chem.msu.su

[*]To whom correspondence should be addressed
[†]Moscow State University
[‡]University of Maryland
[¶]University of Melbourne

Abstract

The structural and spectroscopic properties of the Be^+-H_2 and Be^+-D_2 electrostatic complexes are investigated theoretically. A three dimensional ground-state potential energy surface is generated *ab initio* at the CCSD(T) level and used for calculating the lower rovibrational energy levels variationally. The minimum of the PES corresponds to a well depth of 3168 cm^{-1}, an intermolecular separation of 1.776 Å, with the bond of H_2 subunit being longer by 0.027 Å than for the free molecule. Taking vibrational zero point energy into account, the complexes are predicted to be relatively strongly bound with dissociation energies of 2678 and 2786 cm^{-1} for systems containing para H_2 and ortho D_2, respectively. The ν_{HH} band of Be^+-H_2 is predicted to be red-shifted from the free dihydrogen transition by –323 cm^{-1}, whereas the corresponding shift for Be^+-D_2 is predicted to be –229 cm^{-1}. The dissociation energy of the Be^+-D_2 complex containing para D_2 is predicted to be slightly higher than the energy required to vibrationally excite the D_2 subunit, raising the possibility that the dissociation threshold can be observed in the infrared predissociation spectrum by exciting higher rotational levels in the ν_{DD} manifold.

Introduction

Understanding the interactions of molecular hydrogen with atomic ions is of great interest in many respects. Adsorption of hydrogen on acidic or basic centers of porous materials is a key step of the present-day large-scale industrial chemical process – catalytic hydrogenation/dehydrogenation, and, is expected to be important for tomorrow's hydrogen storage technologies. Two basic parameters, the heat of adsorption and degree of hydrogen bond activation (qualitatively taken as its elongation Δr or vibrational frequency shift $\Delta\nu_{HH}$ with respect to the gas-phase value) are of prime importance for customizing the materials to practical demands. Organometallic chemistry has provided the means to control these parameters over a wide range.[?] In rationally designing new materials the interactions of hydrogen molecule with a bare ion in the gas phase provides a useful reference point and benchmark.

It is therefore not surprising that significant efforts have been devoted to the experimental characterization of dihydrogen containing complexes, as summarized in a recent review.[?] The electrostatic M^+-H_2 and A^--H_2 complexes are formed due to long-range electrostatic and induction forces (charge-quadrupole and charge-induced dipole, to the lowest order). The former largely dictates the equilibrium structure of the complex – T-shaped for cations and linear for anions.[? ?] However, more subtle chemical effects augment the physical ones, and determine large variations of the structural and energetic parameters. These effects are discussed in detail for complexes containing transition metal cations (see, *e.g.*, refs. **? ? ?**) due to their importance for catalysis and the ion-molecular chemistry of *d*-elements.[? ?] The interaction strength, characterized by the well depth D_e or dissociation energy D_0, determines the heat of the complex formation, whereas Δr or $\Delta\nu_{HH}$ are symptomatic of the perturbation to the hydrogen molecule. These quantities are of interest for direct correlations with adsorption properties. Thermochemical methods are convenient for determining binding energies and indeed most of these data originate from clustering equilibrium measurements.[? ? ?] During the last decade, the application of infrared photodissociation spectroscopy has greatly extended our ability to probe the influence of an ion on the hydrogen molecule.[? ?] The IR spectra of M^+-H_2 complexes have been obtained by exciting the $n_{HH} = 0 \rightarrow n_{HH} = 1$ transition of the H_2 diatomic with detection of the M^+ ionic photofragments. The ensuing spectra display rotational substructure that reflects the geometry of the complexes along with providing the frequency shift $\Delta\nu_{HH}$. Generally, spectroscopic methods do not probe the dissociation energy directly. A notable exception is the Cr^+-D_2 complex, for which there is a threshold for photofragmentation at a particular rovibrational level permitting the dissociation energy to be determined more accurately than by thermochemical measurements.[?] Owing to developments in laser ion cooling, another spectroscopic technique that is sensitive to the interaction between dihydrogen and metal cations has recently emerged. Contact of molecular hydrogen with an ultracold trapped single M^+ ion or its Coulomb crystal followed by laser electronic excitation results in formation of MH^+ product ions following reaction on the excited state potential energy surface, see, *e.g.*, refs. **? ? ?** for Be^+ and Mg^+ ions.

Experimental progress has revitalized interest in theoretical studies of the ion-hydrogen interactions. Although the equilibrium structure and harmonic vibrational frequencies have been calculated *ab initio* for a large range of systems,[?] this level of theory is generally inadequate for describing the non-rigid M^+-H_2 complexes. Anharmonicity correction, *e.g.*, within the vibrational self-consistent field method,[?] is essential. Previous experience[? ? ? ?] including our own,[? ? ? ? ? ? ? ?] shows that for the main-group anionic and cationic electrostatic complexes variational rovibrational energy level calculations based on a three-dimensional (3D) potential energy surface (PES) obtained at a high level of the *ab initio* theory with correlation treatment not only reproduces the observed spectral features, but also help fitting of line positions within conventional spectroscopic models, as well as elucidating intensity distributions. To account for the H-H stretching vibration, the diabatic separation of the fast diatomic vibration was found to be a good approximation, thereby reducing the vibrational problem to two dimensions facilitating spectroscopic predictions for high rotational angular momenta J and for metastable levels in the excited $n_{HH} = 1$ manifold. In this paper, we apply this rigorous theoretical methodology for making quantitative predictions on the structure, energetics and spectroscopic constants of the Be^+-H_2 and Be^+-D_2 electrostatic complexes.

Characterizing the interaction between Be^+ and H_2 is an important step for understanding the storage of hydrogen in porous materials with oxidised beryllium centres. Indeed, despite beryllium being a rare and toxic element, Be-based metal-organic frameworks have been synthesized and tested for hydrogen storage properties,[?] and some non-interstital Be-containuing hydrides are actively being studied for the same purpose.[?] Beryllium and its molecules are also of interest for astrophysics and astrochemistry. Its origin in the Universe is controversial.[? ? ?] The BeH molecule and its cation have been identified in comets and stars.[? ?] Despite its low abundance, Be^+ ion is considered as an important astrophysical tracer.

Neutral BeH_2 is a linear symmetric molecule formed by insertion into H_2 bond, as established spectroscopically[? ?] and theoretically.[? ?] In contrast, the Be^+-H_2 electrostatic complex has not yet been characterized experimentally. *Ab initio* calculations were presented in refs. [? ?] and,

most recently, by Page *et al.*[?] The latter work proves that the T-shaped electrostatic complex corresponds to the lowest bound structure (the linear insertion product $HBeH^+$ lies more than 10000 cm^{-1} above) and provides useful data for assessing the present results.

Potential energy surfaces

The interaction energy between the Be cation in its ground ^2S state and the $^1\Sigma_g^+$ hydrogen molecule produces a single ground-state PES of $^2A'$ symmetry. The interaction strength depends on the radial separation and on the orientation of the hydrogen molecule with respect to the intermolecular bond. In the electronic structure calculations we need to represent three degrees of freedom describing the relative positions of the atoms in Be^+-H_2 complex by a discrete grid of points. The geometry of the Be^+-H_2 complex is conveniently described by Jacobi coordinates (r, R, θ). Here, r denotes the internuclear separation in the H_2 molecule, $\boldsymbol{R}$ is the vector from the H_2 center-of-mass to the Be^+ ion that defines the z-axis of the body-fixed (BF) frame, and θ is the angle between $\boldsymbol{r}$ and $\boldsymbol{R}$.

In this section we first describe the electronic structure methods used in the calculations of the ground-state interaction PES, its analytical representation for subsequent bound states calculations and the properties of stationary points. Second, some results for excited-state PESs are briefly mentioned.

Ab initio calculations

The reference wave function for the Be^+-H_2 system for subsequent single-reference coupled-cluster calculations was obtained at the restricted Hartree-Fock (RHF) level. The electronic correlation energy was recovered by partially spin-restricted coupled-cluster method including single and double excitations and non-iterative triple excitations [CCSD(T)].[?] The interaction energy

was calculated within a supermolecular approach:[?]

$$\begin{aligned} V(r,R,\theta) &= E_{\mathrm{Be}^+-\mathrm{H}_2}(r,R,\theta) \\ &- E^{\mathrm{DCBS}}_{\mathrm{Be}^+}(r,R,\theta) - E^{\mathrm{DCBS}}_{\mathrm{H}_2}(r,R,\theta), \end{aligned} \quad (1)$$

where $E_{\mathrm{Be}^+-\mathrm{H}_2}(r,R,\theta)$ is the total energy of the entire complex, while $E^{\mathrm{DCBS}}_{\mathrm{Be}^+}(r,R,\theta)$ and $E^{\mathrm{DCBS}}_{\mathrm{H}_2}(r,R,\theta)$ are the total energies of Be^+ and H_2 monomers, respectively, calculated in the basis set of all constituents – the dimer centred basis set (DCBS). This procedure accounts for the basis set superposition error using the standard counter-poise (CP) correction scheme,[?] but excludes the intramolecular potential energy of H_2 moiety at $R \to \infty$, $U(r)$.

The correlation-consistent aug-cc-pVQZ basis set of the quadruple-zeta quality[?] for hydrogen, extended with additional 3s3p2d2f1g bond functions[?] placed halfway between H_2 center of mass and Be cation, was used for the calculations. For the Be cation, the core-valence correlation was included in coupled-cluster calculations by correlating the electrons on 1*s* orbital. Therefore, the specially adapted aug-cc-pCVQZ basis[?] was employed for this purpose.

The potential was calculated on a discrete grid in which diatomic distance r varies from 1.0 to 2.4 bohr in steps of 0.2 bohr, θ from 0° to 90° in steps of 22.5°, and R varies from 2.5 to 50 bohr in 44 points (with varied step from 0.25, 0.5 to 1.0 bohr for the larger distances). The full 3D PES was obtained by summing the interaction PES $V(r,R,\theta)$ (**??**) and an accurate potential energy curve for the H_2 monomer $U(r)$.[?] All electronic structure calculations were performed with the MOLPRO (ver. 2010.1) program package.[?]

Analytical fit

The analytical representation of the PES was similar to the one used in our previous studies of the Mg^+-H_2 complex.[?] In brief, it implements the reproducing kernel Hilbert space (RKHS) method[?] for fitting the *ab initio* points and extrapolating the PES with the radial kernel corresponding to a R^{-3} long range dependence, see below. The only adaptation this method required for the present

purpose is the size of the Be^+-H_2 *ab initio* grid. The FORTRAN routines for analytical PES generation are available from the authors upon request.

Characterization of the PES

The two-dimensional contour plot of the PES constructed using the RKHS fit in the $X = R\cos\theta$, $Y = R\sin\theta$ Cartesian coordinates at the equilibrium distance of a free hydrogen molecule $r_e(H_2) =$ 0.741 Å is presented in figure **??**. The features of the PES are typical for M^+-H_2 complexes and can be understood as the interplay of the lowest-order long-range forces, namely, the electrostatic charge-quadrupole

$$V_{\rm el} = \Theta q P_2(\cos\theta)/R^3 \tag{2}$$

and the charge-induced dipole induction

$$V_{\rm ind} = -\frac{1}{2}q^2\left[\alpha_0 + \alpha_2 P_2(\cos\theta)\right]/R^4 \tag{3}$$

interactions. Here we used the atomic units (a.u.) and denoted, for H_2, the quadrupole moment as Θ and the isotropic and anisotropic polarizabilities as $\alpha_0 = (\alpha_\parallel + 2\alpha_\perp)/3$ and $\alpha_2 = 2(\alpha_\parallel - \alpha_\perp)/3$, respectively. The charge of the Be^+ ion is $q = +1$ and Θ for H_2 is positive.[?]

For M^+-H_2 complexes, the induction interaction is attractive for all orientations but favours a $\theta = 0$ linear configuration (as $\alpha_\parallel > \alpha_\perp$). The charge-quadrupole interaction is attractive for $\arccos(1/\sqrt{3}) < \theta < \pi/2 + \arccos(1/\sqrt{3})$ with a minimum at $\theta = 90^\circ$, and is repulsive outside this range. At chemically important intermolecular separations ($R > 1$ Å), the minimum in the angle-dependent charge-quadrupole interaction dominates the maximum in the induction interaction and favours a T-shaped M^+-H_2 complex. At the linear configuration ($\theta = 0$), the competition between the charge-quadrupole interaction (which is repulsive) and the induction interaction (which is attractive) leads to appearance of a maximum at long range and the saddle at the shorter distance.

Three stationary points are marked in figure **??** by arrows and characterized in table **??** in terms

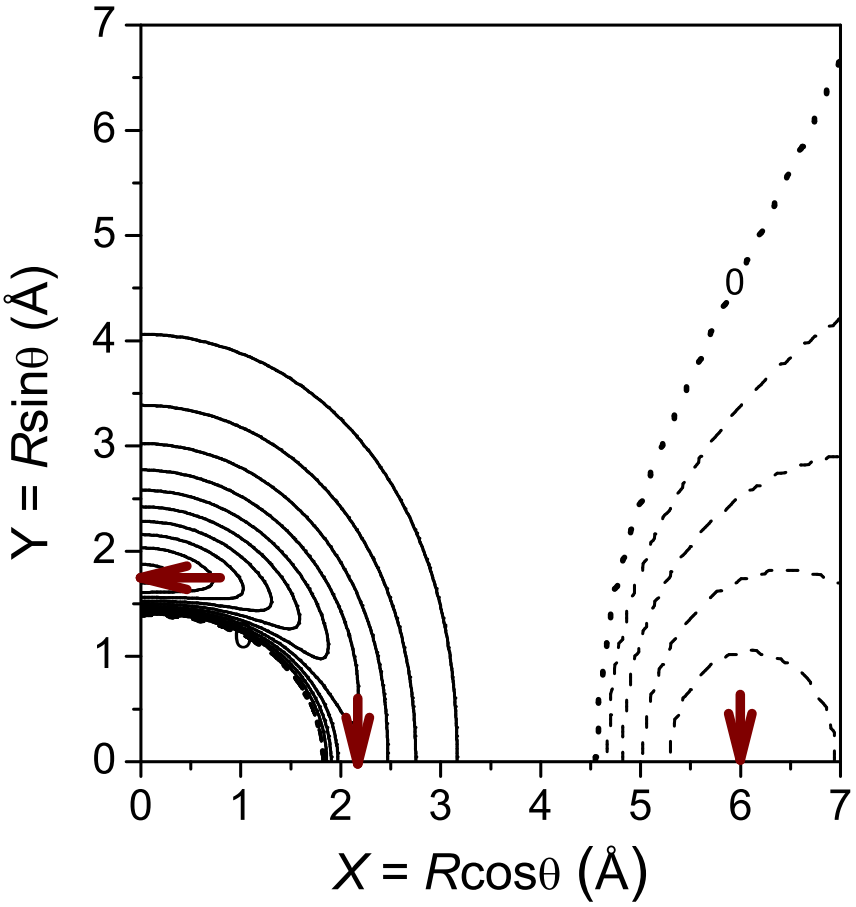

Figure 1: Contour plot of the Be^+-H_2 PES at $r = 0.741$ Å in Cartesian (X,Y) coordinates. Solid lines correspond to negative energy contours from -3000 to -300 cm^{-1}, with the increment of 300 cm^{-1}, dotted line corresponds to zero energy (Be^+ + H_2 dissociation limit), dashed lines correspond to positive contours 5, 10, 15 and 20 cm^{-1}. Arrows indicate the positions of the stationary points, minimum, saddle and maximum, in order of increasing X.

of r and R distances and energy E, the sum of inter- and intramolecular terms V and U, related to its $R \to \infty$ limit, *i.e.*, free Be_+ cation and H_2 molecule at equilibrium. The results for the equilibrium structure (minimum) are in excellent agreement with the calculations by Page *et al.*[?] who used the same basis set for hydrogen, atomic natural orbital basis set for Be and no bond functions in the CCSD(T), CCSDT (full account of triples in the single-reference coupled cluster method), and multi-reference configuration interaction with Davidson correction (MRCI+Q) correlation treatments (CP correction included). Good agreement is also seen for the saddle point, especially if one takes into account the 150 cm^{-1} energy difference between CCSD(T) and MRCI+Q results at equilibrium. These comparisons indicate the good convergence of our *ab initio* scheme and justify the perturbative treatment of triple excitations.

Interaction with the Be^+ ion significantly perturbs the hydrogen molecule. At the equilibrium configuration, the H–H bond is elongated by 0.027 Å (4%) compared to the free molecule. As noted in ref. [?] in relation to the results from ref. [?], this is a record Δr value for main-group cations. The short equilibrium interfragment separation R and large well depth $D_e = -E$ also indicate an unusually strong interaction of the Be^+ with molecular hydrogen.

Numerical solution of the normal mode vibrational problem for the fitted PES gives an H_2 frequency $\nu_{HH}(h) = 4082$ cm^{-1}, shifted to the red by 320 cm^{-1} (7%) with respect to that of the free dihydrogen molecule [hereafter "(h)" indicates harmonic approximation]. Page *et al.*[?] reported an even lower value, 3850 cm^{-1}. This mismatch seems strange in view of the excellent agreement for other parameters. Intermolecular stretching $\nu_s(h)$ and bending $\nu_b(h)$ frequencies for Be^+-H_2 were calculated as 629 and 804 cm^{-1}, respectively. Thus, the dissociation energy corrected for harmonic zero-point energy value $D_0(h)$ amounts to 2452 cm^{-1}. For Be^+-D_2, the harmonic vibrational frequency shift is $\Delta\nu_{DD}(h) = 228$ cm^{-1}, whereas $\nu_s(h) = 484$, $\nu_b(h) = 571$, and $D_0(h) = 2641$ cm^{-1}.

Table 1: Stationary points of the Be^+-H_2 *ab initio* PES. Energies are given with respect to the Be^+ + H_2 dissociation limit.

Method	r, Å	R, Å	E, cm^{-1}
Minimum, $\theta = 90^\circ$			
CCSD(T), this work	0.768	1.776	-3168
CCSD(T)[?]	0.767	1.775	-3154
CCSDT[?]	0.768	1.776	-3170
MRCI+Q, this work	0.767	1.794	-3020
MRCI+Q[?]	0.767	1.774	-3018
Saddle, $\theta = 0$			
CCSD(T), this work	0.761	2.153	-1209
MRCI+Q, this work	0.762	2.174	-1185
MRCI+Q[?]	0.761	2.152	-1070
Maximum, $\theta = 0$			
CCSD(T), this work	0.741	5.923	21

Excited-state PESs: An overview

Despite the calculations by Page *et al.*[?] demonstrating very reasonable agreement between the single-reference CCSD(T) and multi-reference MRCI+Q approaches at the equilibrium configuration, one cannot exclude the failure of the former approach at shorter interfragment distances due to possible interaction with excited electronic states. To check this, we performed the test MRCI+Q calculations using the compact aug-cc-pVTZ basis set and active space consisting of $1s$, $2s$ and $2p$ orbitals for both Be and H centers. No bond functions and CP correction for basis set superposition error were used.

The lowest excited states of the Be^+-H_2 complex arise from the excitation of the ion to its first excited $^2P^\circ$ term[?] by 31000 cm^{-1} (32200 cm^{-1} in our calculations). In the triatomic complex of C_s symmetry, this excitation gives rise to three adiabatic states, $2^2A'$ and $3^2A'$ with electron excitation to in-plane $2p_z$ and $2p_y$ orbitals, and $1^2A''$ associated with out-of-plane $2p_x$ excitation. One-dimensional sections of the corresponding PESs along the R coordinate (r and θ coordinates were optimized for the ground state at each R value) are shown in figure **??**. Both $2^2A'$ and $1^2A''$ PESs are much more attractive than the ground $1^2A'$ one. As a result, avoided crossing of the two lowest $^2A'$ PESs occurs at $R \approx 1.2$ Å, almost at the minimum of the excited curve. For the

ground state, however, the crossing point lies high enough on the repulsive branch to justify the validity of the single-reference CCSD(T) method over the whole range of geometries relevant to the ground-state electrostatic complex and its rovibrational bound states.

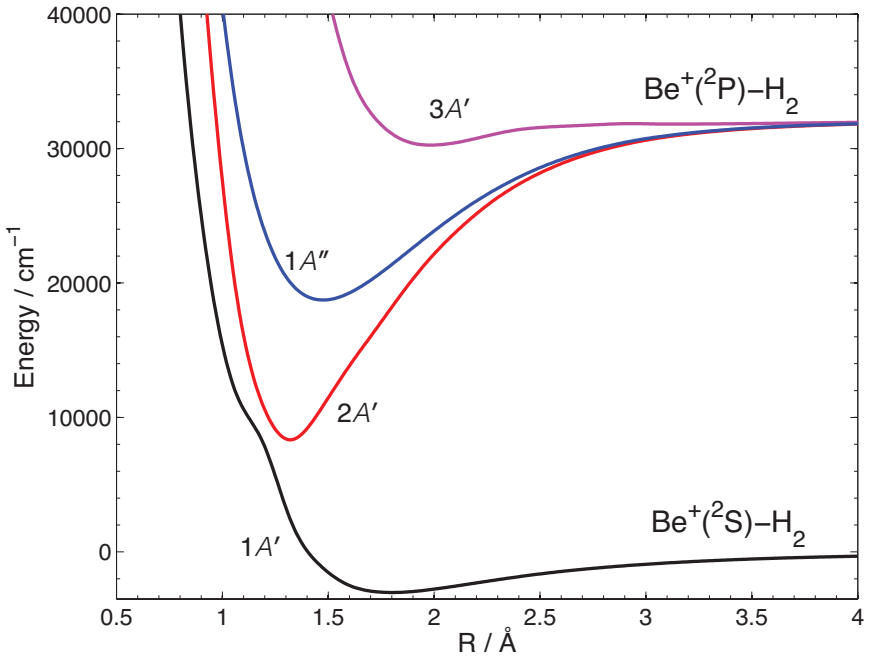

Figure 2: One-dimensional sections of the lowest $Be^+ + H_2$ PESs along the R coordinate (r and θ coordinates were optimized for the ground state at each R value).

The states correlating with the $Be^+(^2P^\circ)$ term are involved in the photoinitiated bond cleavage of molecular hydrogen colliding with Be^+ in Coulomb crystals. Roth *et al.*[?] found that this process has a rate as high as 10^{-9} cm^3/s, which points to a direct barrierless reaction pathway. Assuming that the triatomic complex provides insights into the bimolecular reaction, we computed 2D sections of the excited PESs in r, R coordinates at selected values of θ, as shown in figure **??** for the lowest $2^2A'$ state. The PES is strongly repulsive with respect to formation of the BeH^+ molecular ion. The $\theta = 90^\circ$ panel in the figure shows the contours associated to the minimum region of the ground-state PES. It indicates, in accord with observations,[?] that Be^+ excitation should lead to BeH^+ formation with almost unit probability. One interesting conclusion of this qualitative analysis is the possibility to initiate the process with photon energies much less (by 12000 cm^{-1} for the triatomic complex) than that resonant to the $^2S \rightarrow {}^2P^\circ$ bare ion transition. Our

calculations also allow the exothermicity of the $Be^+(^2P^\circ)$ + $H_2 \rightarrow BeH^+(X^1\Sigma^+)$ + H reaction to be estimated as 2.397 eV. The ground-state reaction should be endothermic by 1.596 eV (*cf.* 1.57 eV, as calculated in ref. **?**).

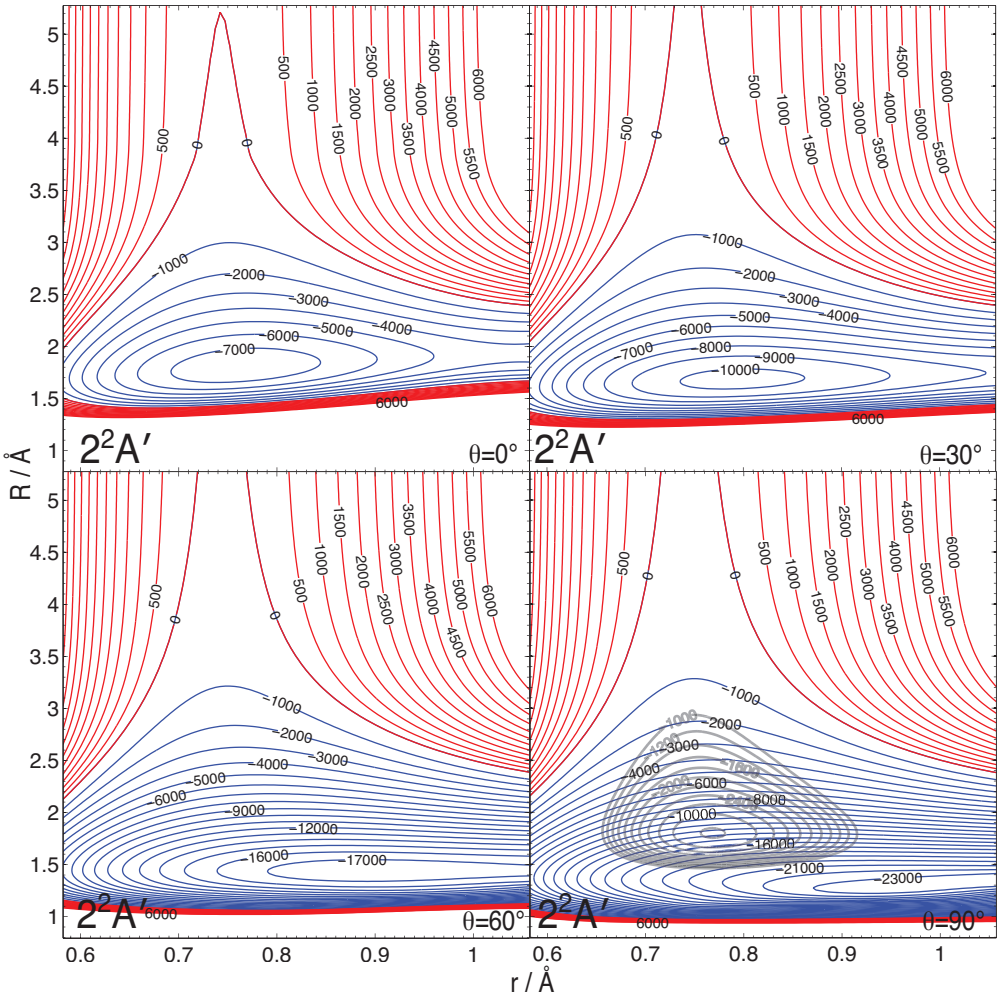

Figure 3: Contour plots of the $2^2A'$ PES at four values of θ angle. The contours are labeled by energies (in cm^{-1}) with respect to the $Be^+(^2P^\circ)$ + $H_2(r = r_e)$ limit. Grey contours on the $\theta = 90^\circ$ panel characterize the minimum region of the ground-state PES and are labeled with respect to $Be^+(^2S)$ + $H_2(r = r_e)$ limit that lie 32200 cm^{-1} below.

One should note that the role of excited states in the Mg^+ + H_2 reactions was carefully analysed by Gianturco and co-workers.**?** More efforts are needed to achieve the same degree of detail for Be^+ case. In the rest of the paper, we concentrate on the ground-state Be^+-H_2 electrostatic complex.

Rovibrational energy levels

Variational method

The RKHS PES was used to calculate the lowest rovibrational energy levels of the Be^{+}-H_2 electrostatic complex using the procedure described in detail in ref. **?**

The total rovibrational Hamiltonian describing the complex in 3D is written in a.u. as

$$\hat{H} = -\frac{1}{2\mu}\frac{\partial^2}{\partial R^2} - \frac{1}{2m}\frac{\partial^2}{\partial r^2} + \frac{(\mathbf{J}-\mathbf{j})^2}{2\mu R^2} + \frac{\mathbf{j}^2}{2mr^2} + U(r) + V(r,R,\theta), \tag{4}$$

where $\mathbf{J}$ and $\mathbf{j}$ are the rotational angular momenta of the complex and of the H_2 moiety, respectively, whereas μ and m are the corresponding reduced masses. The total PES is given as the sum of the unperturbed intermolecular H_2 potential U and intermolecular interaction V in accord with the present *ab initio* approach.

The total wave function is represented by a linear combination of the products of H_2 vibrational χ, radial ϕ and angular Θ basis functions:

$$\Psi_n^{JMp_ip_j} = \sum_w \sum_k \sum_{j\Omega} C_{wkj\Omega}^{Jp_ip_j,n} \chi_w(r)\phi_k(R)\Theta_{j\Omega}^{JMp_ip_j}(\hat{\mathbf{r}}\cdot\hat{\mathbf{R}}), \tag{5}$$

where Ω denotes the absolute value of the projection of $\mathbf{J}$ and $\mathbf{j}$ in the BF frame and M is the projection of $\mathbf{J}$ onto the space-fixed (SF) axis. The χ_w functions are chosen as the wave functions of the free H_2 molecule evaluated numerically:

$$\left[-\frac{1}{2m}\frac{\partial^2}{\partial r^2} + U(r)\right]\chi_w(r) = \varepsilon_w\chi_w(r). \tag{6}$$

Radial ϕ_k functions are also computed numerically by solving similar Schrödinger equation

$$\left[-\frac{1}{2\mu}\frac{\partial^2}{\partial R^2} + V(r=r_e,R,\theta=90^\circ)\right]\phi_k(R) = \varepsilon_w\phi_k(R) \tag{7}$$

with the one-dimensional radial section of the interaction PES at equilibrium value of angle θ. The angular basis $\Theta_{j\Omega}^{JMp_ip_j}$ consists of the symmetrized rigid rotor functions:[?]

$$\Theta_{j\Omega}^{JMp_ip_j}(\hat{\mathbf{r}}\cdot\hat{\mathbf{R}}) = \left[\frac{2J+1}{8\pi(1+\delta_{\Omega 0})}\right]^{1/2}\times \left[D_{M\Omega}^{*J}(\alpha,\beta,0)Y_{j\Omega}(\theta,\varphi)+p_i(-1)^J D_{M-\Omega}^{*J}(\alpha,\beta,0)Y_{j-\Omega}(\theta,\varphi)\right], \tag{8}$$

where $D_{M\Omega}^{*J}(\alpha,\beta,0)$ is the Wigner rotational matrix, which depends on the Euler angles connecting BF and SF frames, and $Y_{j\Omega}(\theta,\varphi)$ is the spherical harmonics describing 3D rotation of H_2 with respect to BF frame. This choice of angular functions fully accounts for the symmetry by means of the parity quantum numbers.[?] The parity index $p_i = \pm$ is connected to the inversion parity p, $p = p_i(-1)^J$, while the permutation parity p_j defines the parity of j ($p_j = +$ for even j's and $p_j = -$ for odd j's). One should note that p_j is connected to the symmetry of the nuclear spin wave function of the monomer, namely, $p_j = +$ for para-hydrogen, pH_2, and ortho-deuterium, oD_2, and $p_j = -$ for oH_2 and pD_2.

Variational solution gives the energies $E_n^{Jp_ip_j}$ and expansion coefficients C in eq.(**??**) for the levels associated with H_2 fragment in its ground vibrational state $n_{HH} = 0$. Convergence tests showed that a basis set consisting of 4 vibrational, 10 radial and 12 angular functions provides the 6 lowest energy levels of each $J^{p_ip_j}$ block with 0.02 cm^{-1} accuracy.

For infrared photodissociation spectroscopy of M^+-H_2 complexes, transitions are probed by exciting the $n_{HH} = 0 \rightarrow n_{HH} = 1$ excitation of the H_2 moiety in the complex and detecting M^+ fragments.[?] The levels associated with $n_{HH} = 1$ state are metastable and cannot be obtained using the expansion (**??**) over the square-integrable radial functions. In order to estimate the shift of the n_{HH}=0$\rightarrow$ n_{HH}=1 transitions, we used, as before,[?] the so-called vibrational diabatic decoupling approximation.[?] This assumes that the fast vibration of the H_2 moiety is not affected by the slow intermolecular dynamics, so its wave function is given by the solution of eq.(**??**) for certain n_{HH}. The intermolecular motion is therefore determined by the the effective two-dimensional (2D)

Hamiltonian

$$\hat{H}_{n_{HH}} = -\frac{1}{2\mu}\frac{\partial^2}{\partial R^2} + \frac{(\mathbf{J}-\mathbf{j})^2}{2\mu R^2} + B_{n_{HH}}\mathbf{j}^2 + V_{n_{HH}}(R,\theta) + \varepsilon_{n_{HH}}, \tag{9}$$

where $B_{n_{HH}} = \langle\chi_{n_{HH}}|r^{-2}|\chi_{n_{HH}}\rangle/2m$, $V_{n_{HH}} = \langle\chi_{n_{HH}}|V(r,R,\theta)|\chi_{n_{HH}}\rangle_r$. This approximation is equivalent to retaining the single $w = n_{HH}$ term in eq.(**??**). The variational solution is obtained using the same radial and angular basis sets as described above and provides the same accuracy.

Note that the spin-rotation interaction is ignored. As argued and found for the Mg^+-H_2 complex, the corresponding splitting is small comparing the typical linewidth in the IR photodissociation spectrum.[**?**]

Three dimensional calculations

The results of the 3D calculations on the lowest energy levels of the four individual species for $J = 0$ and 1 are presented in the table **??**. The levels of the complexes containing pH_2 and oD_2 appear in the 0^{++} and 1^{++} symmetry blocks, whereas those of oH_2 and pD_2 are in the 1^{+-} and 0^{+-} blocks. All energies are related to the absolutely lowest dissociation limit, Be^++pH_2 ($n_{HH} = 0, j = 0$) or Be^++oD_2 ($n_{DD} = 0, j = 0$). However, since the Be^+-oH_2 and Be^+-pD_2 complexes can only dissociate to give the rotationally excited $j = 1$ diatomic fragment, their dissociation energy should be corrected by the rotational energy of the product molecule, 118.67 cm^{-1} for H_2 and 59.83 cm^{-1} for D_2. As a result, the Be^+-pH_2 complex has $D_0 = 2678$ cm^{-1}, whereas for Be^+-oH_2 complex it is $D_0 = 2727$ cm^{-1}. Dissociation energies of the deuterated complexes are larger due to reduced vibrational zero-point energy, $D_0 = 2786$ cm^{-1} for Be^+-oD_2 and $D_0 = 2812$ cm^{-1} for Be^+-pD_2. This trend – the complexes containing the even-j spin-isomers (pH_2, oD_2) have lower absolute energy than complexes containing the odd-j spin-isomers (oH_2, pD_2), but are effectively less stable – is common for all electrostatic complexes studied so far.[**?**] Using the harmonic approximation for the vibrational frequencies and zero-point energy leads to D_0 being underestimated by 5-8 %.

For each level, table **??** also provides vibrationally-averaged distances. The $\langle r\rangle$ and $\langle R\rangle$ quan-

tities were computed as the expectation values of r and R with the wave function (**??**), whereas $\bar{r}$ and $\bar{R}$ were obtained from the expectation values of r^{-2} and R^{-2}, in a manner closer to spectroscopic structure determination. Intramolecular parameters $\langle r \rangle$ and $\bar{r}$ differ between each other by *ca.* 0.016 Å for hydrogen and 0.012 Å for deuterium. Computing the same quantities for free hydrogen molecule, $\langle r \rangle = 0.766$ and $\bar{r} = 0.751$ Å, we estimated the elongation of the H–H bond in the ground-state complexes as 0.012-0.014 Å, half that obtained from the equilibrium structure, see table **??**. The same differences apply to the D_2 stretching motion.

In contrast, vibrationally-averaged intermolecular distances $\langle R \rangle$ and $\bar{R}$ are much larger (*e.g.*, by 0.068 and 0.052 Å for the pH_2 complex, 0.050 and 0.039 Å for the oD_2 complex) than the equilibrium R_e value. This explains the counterintuitive contraction of the vibrationally-averaged H–H and D–D bond lengths with respect to equilibrium ones in the complex. When averaged over the zero-point excursions in the intermolecular modes, the intermolecular distance is longer than the equilibrium distance and therefore the Be^+ ion perturbs the H_2 molecule less than at the equilibrium separation. For the same reason, intermolecular excitations that on average move the fragments further apart lead to a slight contraction of H_2 and D_2 distances compare to the equilibrium separations. Indeed, table **??** shows a clear inverse correlation of the averaged r and R values.

Vibrationally-averaged distances R can be used, together with the nodal patterns of the rovibrational wave functions, to assign the lowest energy levels according to the number of quanta (n_s, n_b) for decoupled intermolecular stretching (ν_s) and bending (ν_b) vibrations. Using the levels and their assignments from table **??**, one can calculate the fundamental stretching frequencies of the Be^+-pH_2 and Be^+-oD_2 complexes as 532 and 427 cm^{-1}, respectively, and estimate their harmonic analogs as 598 and 467 cm^{-1}. The frequencies $\nu_s(h)$ determined by the normal mode analysis are 4-7% higher.

For symmetry reason, only even bending excitations are allowed within the symmetry block that contains the ground level. The $2\nu_b$ excitation energies amounts to 1218 and 968 cm^{-1} for pH_2 and oD_2 complexes, respectively. The singly excited bending levels of the complexes with

oH_2 and pD_2 appear in the 0^{+-} block (673 cm^{-1} and 512 cm^{-1} above the ground state for Be^+-H_2 and Be^+-D_2, respectively), whereas those of pH_2 and oD_2 appear in the 1^{++} and 1^{-+} blocks as the components of asymmetry doublets slightly split by Coriolis interaction. The energies of one component are given in table **??**. Comparison with harmonic $\nu_b(h)$ frequencies (804 and 571 cm^{-1} for Be^+-H_2 and Be^+-D_2, respectively) indicates large anharmonicity of the bending motion. Bending excitation increases the interfragment distance and contracts the diatomic bond length, but understandably to a lesser extent than does the stretching excitation.

Variational results for all parity blocks with $J = 0-4$ for Be^+-H_2 and $J = 0-2$ for Be^+-D_2 were fitted using an A-reduced Watson Hamiltonian to determine effective spectroscopic constants for the $n_{HH} = 0$ and $n_{DD} = 0$ levels. Parameters are compiled in table **??**. As observed for other similar floppy atom-diatomic complexes, although the lower energy levels are adequately fit by the standard Watson Hamiltonian, the spectroscopic constants are influenced by the large amplitude vibrational motions (particularly the intermolecular bend vibration) and the A constant in particular is difficult to relate to any sensible geometrical structure.

Intramolecular vibrational frequency shift

To estimate the shifts in the vibrational frequencies of H_2 and D_2 molecules engaged in the complexes, 2D variational calculations were performed. For the transitions connecting the lowest rovibrational levels of the initial $n_{HH} = 0$ and final $n_{HH} = 1$ manifolds, the excitation energies and the line intensities were computed, as described elsewhere.[?] The results for the most intense transitions (the lowest R branch transitions) from the ground levels of each complex (selection rules are $J'' - J' = 0, \pm 1$, $p'_i = -p''_i$, $p'_j = p''_j$) are presented in table **??**. The energies of the initial E'' and final E' levels are given with respect to the ground vibrationally-adiabatic asymptotic limit, $Be^+ + H_2$ ($n_{HH} = 0, 1$, $j = 0$) or $Be^+ + D_2$ ($n_{DD} = 0, 1$, $j = 0$). It should be noted that there is a significant difference (82 cm^{-1}, or 3% of D_e) between the $n_{HH} = 0$ energies calculated within the 3D approach (*cf.* table **??**) and the 2D approximation. In the former, inclusion of the wave functions describing vibrational excitations of the molecular fragment in the basis set effectively

Table 2: Lowest rovibrational energy levels of the Be^+ electrostatic complexes with the nuclear spin-isomers of H_2 and D_2. Energies are given with respect to the ground dissociation limits with H_2/D_2 molecule in its ground state $n_{HH} = 0, j = 0$.

n	(n_s, n_b)	E, cm^{-1}	$\langle r \rangle$, Å	$\bar{r}$, Å	$\langle R \rangle$, Å	$\bar{R}$, Å
		Be^+-pH_2, $J^{p_i p_j} = 0^{++}$				
0	(0,0)	-2677.87	0.780	0.763	1.844	1.828
1	(1,0)	-2146.01	0.779	0.762	1.950	1.903
2	(2,0)	-1680.60	0.777	0.761	2.073	1.991
3	(0,2)	-1460.35	0.779	0.762	1.956	1.926
4	(3,0)	-1280.53	0.776	0.760	2.219	2.095
		Be^+-pH_2, $J^{p_i p_j} = 1^{++}$				
0	(0,1)	-1910.08	0.780	0.763	1.869	1.888
		Be^+-oH_2, $J^{p_i p_j} = 1^{+-}$				
0	(0,0)	-2608.63	0.780	0.763	1.843	1.828
1	(1,0)	-2074.22	0.779	0.762	1.949	1.903
2	(2,0)	-1606.18	0.777	0.761	2.073	1.990
3	(0,2)	-1285.41	0.779	0.762	1.935	1.909
4	(3,0)	-1204.00	0.776	0.760	2.218	2.094
		Be^+-oH_2, $J^{p_i p_j} = 0^{+-}$				
0	(0,1)	-2005.54	0.779	0.763	1.893	1.872
		Be^+-oD_2, $J^{p_i p_j} = 0^{++}$				
0	(0,0)	-2786.48	0.773	0.760	1.826	1.815
1	(1,0)	-2359.62	0.772	0.760	1.906	1.871
2	(2,0)	-1973.51	0.771	0.759	1.995	1.934
3	(0,2)	-1818.53	0.772	0.760	1.898	1.879
4	(3,0)	-1627.82	0.770	0.758	2.096	2.006
		Be^+-oD_2, $J^{p_i p_j} = 1^{++}$				
0	(0,1)	-2234.38	0.772	0.760	1.857	1.843
		Be^+-pD_2, $J^{p_i p_j} = 1^{+-}$				
0	(0,0)	-2752.58	0.773	0.761	1.826	1.815
1	(1,0)	-2325.31	0.772	0.760	1.906	1.871
2	(2,0)	-1938.76	0.771	0.759	1.995	1.934
3	(0,2)	-1765.34	0.772	0.760	1.894	1.876
4	(3,0)	-1592.65	0.770	0.758	2.096	2.006
		Be^+-pD_2, $J^{p_i p_j} = 0^{+-}$				
0	(0,1)	-2274.42	0.772	0.760	1.858	1.844

Table 3: Theoretical spectroscopic constants for Be^+-H_2 and Be^+-D_2 obtained by fitting the calculated energy levels derived from the PES presented in the current work to a Watson A-reduced Hamiltonian. Units for all parameters are cm^{-1}.

	Be^+-H_2[a]	Be^+-D_2[b]
A	66.198(1)	32.1316(8)
B	3.0517(5)	1.8359(5)
C	2.8542(5)	1.7093(5)
$\overline{B}$	2.95295	1.7726(5)
$\Delta_J \times 10^4$	3.0(1)	1.0(2)
$\Delta_{JK} \times 10^3$	-7.15(2)	-2.70(2)

[a] from fits to K_a=0 and 1, J=0-4 levels;
[b] from fits to K_a=0 and 1, J=0-2 levels.

allows it to stretch, ensuring a better sampling of the minimum region of the PES. In contrast, the 2D approximation keeps the diatomic subunit essentially unperturbed.

According to the 2D method, the vibrational frequency shift originates from the difference in effective two-dimensional PESs that correspond to distinct vibrational states of the diatomic molecule, *i.e.*, it results from the influence of the diatomic vibrational excitation on the intermolecular interaction. The predicted band shifts, based on fitting the $n_{HH} = 0$ and 1 2D levels to an A-reduced Watson Hamiltonian, are $\Delta\nu_{HH} = -322.9$ cm^{-1} for Be^+-H_2 and $\Delta\nu_{DD} = -228.6$ for Be^+-D_2. The difference in the origins for the K_a=0-0 and K_a=1-1 sub-bands, which are due to distinct nuclear spin-isomers, is predicted to be $\Delta A = 3.4$ cm^{-1} for Be^+-H_2 and $\Delta A = 1.2$ cm^{-1} for Be^+-D_2, and should easily be resolvable in their respective infrared photodissociation spectra. The shifts from the 2D analysis correspond nicely to the results of the normal mode analysis, $\Delta\nu_{HH}(h) = 320$ and $\Delta\nu_{DD}(h) = 228$ cm^{-1}. Note that the harmonic shift is viewed as a consequence of the deformation of the diatomic potential under the influence of the ion.

Discussion

Information is available for a broad range of electrostatic complexes with various metal and semi-metal cations[??] allowing one to draw qualitative correlations between their bonding properties

Table 4: Results of the 2D calculations on the lower $n_{HH/DD} = 0 \rightarrow n_{HH/DD} = 1$ R-branch transitions for the Be^+ electrostatic complexes with the nuclear spin-isomers of H_2 and D_2. Initial E'' and final E' energies are given with respect to the dissociation limits with H_2/D_2 molecule in its rotational ground state $n_{HH/DD} = 0, j'' = 0$ and $n_{HH/DD} = 1, j' = 0$, respectively.

Complex	$J''p_i''p_j'' \rightarrow J''p_i''p_j''$	E'', cm^{-1}	E', cm^{-1}	$\Delta\nu_{HH/DD}$, cm^{-1}
Be^+-pH_2	$0^{++} \rightarrow 1^{-+}$	-2596.05	-2913.03	-316.98
Be^+-oH_2	$1^{+-} \rightarrow 2^{--}$	-2526.65	-2840.95	-314.30
Be^+-oD_2	$0^{++} \rightarrow 1^{-+}$	-2703.18	-2928.22	-225.04
Be^+-pD_2	$1^{+-} \rightarrow 2^{--}$	-2669.22	-2891.76	-222.54

and parameters characterizing the hydrogen bond activation. Our present results actually complete the first two rows of the I, II and III groups of the Periodic table making it possible to compare the corresponding complexes on (practically) the same footing. Table **??** summarizes the main parameters of the pH_2 complexes involving the Li, Be, B, Na, Mg and Al cations. Most of the data were taken from table 2 in ref. **?** and include the results of experimental IR photodissociation spectroscopy and theoretical results obtained using the variational energy level calculations based on *ab initio* PESs (refs. **? ?** for Li^+-H_2, ref. **?** for B^+-H_2, ref. **?** for Na^+-H_2, ref. **?** and ref. **?** for Al^+-H_2). The D_0 values from clustering equilibrium measurements are also given.**? ? ?** In addition to structural and spectroscopic parameters, table **??** presents Δq values, the partial charge transfer from H_2 molecule calculated at equilibrium geometry using the natural bond orbital (NBO) analysis.**?** Data from ref. **?** were obtained at the CCSD(T) level with aug-cc-pVTZ basis set, whereas present calculations used the same basis with MRCI+Q method.

Comparison of experimental and theoretical data provided in table **??** allows an indirect assessment of the present theoretical approach. It shows that variational calculations with the CCSD(T) PESs effectively reproduces dissociation energies (B^+-H_2 might seem as exception, but the equilibrium measurements are likely related to the ortho-H_2 complex with $D_0 = 1298$ cm^{-1}, see discussion in ref. **?**) and interfragment distances R_0 (though different definitions, $\langle R \rangle$ or $\bar{R}$, are used in table **??**). As well, the 2D variational approach tend to underestimate the hydrogen vibrational frequency shift by 4-8% (table **??**). A similar discrepancy might be expected for the shifts obtained here for the Be^+-H_2 and Be^+-D_2 complexes.

Short range approach of the M^+ ion to the H_2 molecule in the T-shaped configuration results in Pauli repulsion between electrons in the σ_g bonding orbital and the valence electrons on the M^+ cation. For Be^+-H_2, the repulsion can be mitigated through hybridisation of the $2s$ and $2p_z$ orbitals, shifting electron density away from the intermolecular region to the opposite side of the Be^+ cation. The Δq values provide a clue for assessing this effect regardless to their sensitivity to the *ab initio* scheme. Table **??** indicates that hybridisation plays important role in the stabilization of the Be^+-H_2 complex. The same sort of hybridisation occurs for Mg^+-H_2, but the larger energy gap between $2s$ and $2p_z$ orbitals (4.22 eV *vs.* 3.96 eV for Be^+) strongly suppresses it leading to a short intermolecular bond and high binding energy for the Be^+-H_2 complex.

Inspection of table **??** shows that for the ions studied so far, Be^+ forms the strongest bond to H_2 and leads to the largest deformation of the attached hydrogen molecule. Variation of the structural, vibrational and energetic parameters moving down the Periodic table clearly reflects the weakening of the intermolecular bond, due to increasing radius of the ion, or, equivalently, by increasing exchange repulsion. However, the variations are different within each group. For example, the interfragment distance increases and the dissociation energy drops from Be^+ to Mg^+ much more than from Li^+ to Na^+, so already at the second row alkali metal ion binds to dihydrogen more strongly than do alkailine-earth metal ion. Surprisingly, the perturbation of the H_2 diatomic does not reflect the same trend: both the H–H bond elongation and vibrational frequency shift are larger for Mg^+-H_2 than for Na^+-H_2. The variations for B^+-H_2 and Al^+-H_2 lie between the Li–Na and Be–Mg extremes.

The present results should be useful for guiding future infrared photodissociation investigations. We predict that the bands associated with complexes should be red shifted from the H_2 and D_2 fundamental vibrational transitions by 315 and 220 cm^{-1}, respectively. Complexes with D_2 may provide a particularly interesting case because the dissociation energies, for Be^+-pD_2 and Be^+-oD_2 (2753 and 2786 cm^{-1}, respectively) are close to the $n_{DD} = 0 \rightarrow n_{DD} = 1$ transition energy (2769 cm^{-1}). This means that, particularly for Be^+-oD_2, some of the lower rotational levels associated with upper $n_{DD} = 1$ manifold may actually be bound rather than metastable and may

not appear in the photodissociation spectrum. Such threshold effects were observed for the Cr^+-D_2 complexes and were used to deduce an accurate dissociation energy.[?] Therefore, an experimental investigation of the Be^+-D_2 complex would be extremely interesting for assessing the theoretical methodology and providing benchmark binding energy data.

Even though the splitting between the transitions of the complexes formed by distinct nuclear spin-isomers of hydrogen and deuterium is much larger than the typical spectral resolution, transitions associated with pH_2 are usually difficult to detect. The reason is the quite large difference in stability of the M^+-oH_2 and M^+-pH_2 complexes (predicted to be $\sim$50 cm^{-1} for Be^+-H_2). As a result, the equilibrium of the ortho/para ligand exchange should be strongly shifted towards the oH_2 complex, as explained in detail in ref. **?** . Indeed, the 40 cm^{-1} difference in stability of Mg^+-oH_2 and Mg^+-pH_2 made it impossible to discern the transitions of the latter complexes above the attainable signal-to-noise ratio.[?] The analogous difference for Be^+-oD_2 and Be^+-pD_2 is only 25 cm^{-1} making it more favorable for detecting complexes containing both nuclear spin isomers, again in agreement with the Mg^+ case. Finally, one should mention that it is impossible to obtain the A rotational constant (and an estimate of the H-H bond length) from analysis of the parallel ν_{HH} stretch band.[?] Our present calculations should provide a reliable estimate.

Table 5: Main parameters of the selected electrostatic complexes formed by cations and H_2, theory/experiment. See text for the sources.

Parameter	Li^+-H_2	Be^+-H_2	B^+-H_2	Na^+-H_2	Mg^+-H_2	Al^+-H_2
D_0, cm^{-1}	1732/–	2678/–	1254/1330±70	842/860±70	614/–	473/470±50
R_0, Å	–/2.06	1.83/–	2.28/2.26	2.51/2.49	2.73/2.72	3.07/3.04
Δr, Å	0.010/–	0.027/–	0.014/–	0.006/–	0.008/–	0.005/–
$\Delta\nu_{HH}$, cm^{-1}	–/108	323/–	204/222	64/67	102/106	62/66
Δq, a.u.	–	0.051	0.031	–	0.007	–
Δq, a.u.[?]	0.006	–	0.022	0.003	0.009	0.003

Summary and Conclusions

1. A new RKHS interaction potential energy surface has been developed for the Be^+-H_2 electrostatic complex based on the CCSD(T) approach using the aug-cc-pVQZ basis set extended with additional 3s3p2d2f1g bond functions placed halfway between H_2 center of mass and Be cation.

2. The PES is used to calculate the energies and wave functions for the rovibrational states of Be^+-H_2 and Be^+-D_2 being combined with the accurate isotopic-invariant dihydrogen potential. Effective dissociation energies for Be^+-pH_2 and Be^+-oH_2 are predicted to be 2678 and 2727 cm^{-1}, respectively. Dissociation energies for Be^+-oD_2 and Be^+-pD_2 are slightly larger due to reduced vibrational zero-point energy, and are 2786 and 2812 cm^{-1}, respectively.

3. Based on 2D rovibrational calculations, the ν_{HH} band of Be^+-H_2 is predicted to be shifted by -323 cm^{-1} with respect to the band of the free H_2 molecule, while the corresponding shift for Be^+-D_2 is -229 cm^{-1}.

4. The calculations show that Be^+ is attached more strongly to H_2 than neighbouring cations (Li^+ and B^+) and that it affects the the vibrational frequency and bond length of dihydrogen more profoundly than its neighbours.

5. The Be^+-D_2 system is predicted to exhibit threshold features in its infrared predissociation spectrum as the dissociation energy is comparable to the energy of the ν_{DD} stretch mode. It is likely that there is a threshold for dissociation at a particular J level in the $n_{DD} = 1$ manifold.

Acknowledgement

This work was supported by Russian Foundation for Basic Research under project No. 14-03-00422 and the Australian Research Council's Discovery Project funding scheme (Project Number DP120100100).

References

(1) Kubas, G.J. Fundamentals of H_2 Binding and Reactivity on Transition Metals Underlying Hydrogenase Function and H_2 Production and Storage. *Chem. Rev.* **2007**, *107*, 4152-4205.

(2) Dryza, V.; Bieske, E.J. Non-Covalent Interactions between Metal Cations and Molecular Hydrogen: Spectroscopic Studies of M^+–H_2 Complexes. *Int. Rev. Phys. Chem.* **2013**, *32*, 559-587.

(3) Bieske, E.J. Spectroscopic Studies of Anion Complexes and Clusters: A Microscopic Approach to Understanding Anion Solvation. *Chem. Soc. Rev.* **2003**, *32*, 231-237.

(4) Maître, P.; Bauschlicher, C.W. Theoretical Study of the Hydrogen-Metal Complex (H_2-ML^+) Binding Energies. *J. Phys. Chem.* **1993**, *97*, 11912-11920.

(5) Kemper, P.R.; Bushnell, J.E.; Bowers, M.T.; Gellene, G.I. Binding between Ground-State Aluminum Ions and Small Molecules: $Al^+\cdot(H_2/CH_4/C_2H_2/C_2H_4/C_2H_6)_n$. Can Al^+ Insert into H_2? *J. Phys. Chem.* **1998**, *102*, 8590-8597.

(6) Bushnell, J.E.; Kemper, P.R.; Van Koppen, P.; Bowers, M.T. Mechanistic and Energetic Details of Adduct Formation and σ-Bond Activation in $Zr^+(H_2)_n$ Clusters. *J. Phys. Chem. A* **2001**, *105*, 2216-2224.

(7) Armentrout, P.B.; Beauchamp, J.L. The Chemistry of Atomic Transition-Metal Ions: Insight into Fundamental Aspects of Organometallic Chemistry. *Acc. Chem. Res.* **1989**, *22*, 315-321.

(8) Armentrout, P.B. Periodic Trends in the Reactions of Atomic Ions with Molecular Hydrogen. *Int. Rev. Phys. Chem.* **1990**, *9*, 115-148.

(9) Kemper, P.R.; Bushnell, J.E.; von Helden, G.; Bowers, M.T. $Co^+\cdot(H_2)_n$ Clusters: Binding Energies and Molecular Parameters. *J. Phys. Chem.* **1993**, *97*, 52-58.

(10) Bushnell, J.E.; Kemper, P.R.; Bowers, M.T. $Na^+/K^+\cdot(H_2)_{1,2}$ Clusters: Binding Energies from Theory and Experiment. *J. Phys. Chem.* **1994**, *98*, 2044-2049.

(11) Kemper, P.R.; Bushnell, J.E.; Weis, P.; Bowers, M.T. Cluster-Assisted Thermal Energy Activation of the H–H σ Bond in H_2 by Ground State $B^+(^1S_0)$ Ions: Overcoming a 77 kcal/mol Barrier. *J. Am. Chem. Soc.* **1998**, *120*, 7577-7584.

(12) Dryza, V.; Poad, B.L.G.; Bieske, E.J. Attaching Molecular Hydrogen to Metal Cations: Perspectives from Gas-Phase Infrared Spectroscopy. *Phys. Chem. Chem. Phys.* **2012**, *14*, 14954-14965.

(13) Dryza, V.; Bieske, E.J. The Cr^+–D_2 Cation Complex: Accurate Experimental Dissociation Energy, Intermolecular Bond Length, and Vibrational Parameters. *J. Chem. Phys.* **2009**, *131*, 164303.

(14) Roth, B.; Blythe, P.; Wenz, H.; Daerr, H.; Schiller, S. Ion-Neutral Chemical Reactions between Ultracold Localized Ions and Neutral Molecules with Single-Particle Resolution. *Phys. Rev. A* **2006**, *73*, 042712.

(15) Staanum, P.F.; Højbjerre, K.; Wester, R.; Drewsen, M. Probing Isotope Effects in Chemical Reactions Using Single Ions. *Phys. Rev. Lett.* **2008**, *100*, 243003.

(16) Satta, M.; Marqués-Mijares, M.; Yurtsever, E.; Bovino, S.; Gianturco, F.A. $Mg^+(^2S)$ and $Mg^+(^2P)$ in Reaction with $H_2(^1\Sigma_g^+)$: A Description of the Energy Surfaces Explaining the Mechanisms. *Int. J. Mass. Spectrom.* **2013**, *351*, 47-55.

(17) De Silva, N.; Njegic, B.; Gordon, M.S. Anharmonicity of Weakly Bound M^+-H_2 Complexes. *J. Phys. Chem. A* **2011**, *115*, 3272-3278.

(18) Alexander, M.H. Theoretical Investigation of the Lower Bend-Stretch States of the Cl^-H_2 Anion Complex and its Isotopomers. *J. Chem. Phys.* **2003**, *118*, 9637-9642.

(19) Martinazzo, R.; Tantardini, G.F.; Bodo, E.; Gianturco, F.A. Accurate Potential Energy Surfaces for the Study of Lithium-Hydrogen Ionic Reactions. *J. Chem. Phys.* **2003**, *119*, 11241-11248.

(20) Bulychev, V.P.; Bulanin, K.M.; Bulanin, M.O. Theoretical Study of the Spectral and Structural Parameters of van der Waals Complexes of the Li^+ Cation with the H_2, D_2, and T_2 Isotopomers of the Hydrogen Molecule. *Opt. Spectrosc.* **2004**, *96*, 205-216.

(21) Sanz, C.; Bodo, E.; Gianturco, F.A. Energetics and Structure of the Bound States in a Lithium Complex: The $(LiH_2)^+$ Electronic Ground State. *Chem. Phys.* **2005**, *314*, 135-142.

(22) Buchachenko, A.A.; Grinev, T.A.; Kłos, J.; Bieske, E.J.; Szczęśniak, M.M.; Chałasiński, G. Ab Initio Potential Energy and Dipole Moment Surfaces, Infrared Spectra, and Vibrational Predissociation Dynamics of the $^{35}Cl^-...H_2/D_2$ Complexes. *J. Chem. Phys.* **2003**, *119*, 12931-12945.

(23) Thompson, C.D.; Emmeluth, C.; Poad, B.L.J.; Weddle, G.H.; Bieske, E.J. Rotationally Resolved Infrared Spectrum of the Li^+–D_2 Cation Complex. *J. Chem. Phys.* **2006**, *125*, 044310.

(24) Grinev, T.A.; Buchachenko, A.A.; Kłos, J.; Bieske, E.J. Ab Initio Potential Energy Surface, Infrared Spectra, and Dynamics of the Ion-Molecule Complexes between Br^- and H_2, D_2, and HD. *J. Chem. Phys.* **2006**, *125*, 114313.

(25) Emmeluth, C.; Poad, B.L.J.; Thompson, C.D.; Weddle, G.H.; Bieske, E.J.; Buchachenko, A.A.; Grinev, T.A.; Kłos, J. The Al^+–H_2 Cation Complex: Rotationally Resolved Infrared Spectrum, Potential Energy Surface, and Rovibrational Calculations. *J. Chem. Phys.* **2007**, *127*, 164310.

(26) Poad, B.L.J.; Wearne, P.J.; Bieske, E.J.; Buchachenko, A.A.; Bennet, D.I.G.; Kłos, J.; Alexander, M.H. The Na^+–H_2 Cation Complex: Rotationally Resolved Infrared Spectrum, Potential Energy Surface, and Rovibrational Calculations. *J. Chem. Phys.* **2008**, *129*, 184306.

(27) Dryza, V.; Bieske, E.J.; Buchachenko, A.A.; Kłos, J. Potential Energy Surface and Rovibrational Calculations for the Mg^+–H_2 and Mg^+–D_2 Complexes. *J. Chem. Phys.* **2011**, *134*, 044310.

(28) Poad, B.L.J.; Dryza, V.; Kłos, J.; Buchachenko, A.A.; Bieske, E.J. Rotationally Resolved Infrared Spectrum of the Na^+-D_2 Complex: An Experimental and Theoretical Study. *J. Chem. Phys.* **2011**, *134*, 214302.

(29) Poad, B.L.J.; Dryza, V.; Buchachenko, A.A.; Kłos, J.; Bieske, E.J. Properties of the B^+-H_2 and B^+-D_2 Complexes: A Theoretical and Spectroscopic study. *J. Chem. Phys.* **2012**, *137*, 124312.

(30) Sumida, K.; Hill, M.R.; Horike, S.; Daily, A.; Long, J. Synthesis and Hydrogen Storage Properties of $Be_{12}(OH)_{12}$(1,3,5-benzenetribenzoate)$_4$. *J. Am. Chem. Soc.* **2009**, *131*, 15120-15121.

(31) Grochala, W.; Edwards, P.P. Thermal Decomposition of the Non-Interstitial Hydrides for the Storage and Production of Hydrogen. *Chem. Rev.* **2004**, *104*, 1283-1316.

(32) Tytler, D.; O'Meara, J.M.; Suzuki, N.; Lubin, D. Review of Big Bang Nucleosynthesis and Primordial Abundances. *Phys. Scripta*. **2000**, *T85*, 12-31.

(33) King, J.R. The Galactic Evolution of Beryllium and Boron Revisited. *Astron. J.* **2001**, *122*, 3115-3135.

(34) Pospelov, M.; Pradier, J. Primordial Beryllium as a Big Bang Calorimeter. *Phys. Rev. Lett.* **2011**, *106*, 121305.

(35) Sauval, A.J.; Tatum, T.B. A Set of Partition Functions and Equilibrium Constants for 300 Diatomic Molecules of Astrophysical Interest. *Astrophys. J. Suppl. Ser.* **1984**, *56*, 193-209.

(36) Singh, M. Thirty-One New Diatomic Molecules in Cosmic Objects Spectra. *Astrophys. Space Sci.* **1988**, *104*, 421-427.

(37) Bernath, P.F.; Shayesteh, A.; Tereszchuk, K.; Colin, R. The Vibration-Rotation Emission Spectrum of Free BeH_2. *Science* **2002**, *297*, 1323-1324.

(38) Shayesteh, A.; Tereszchuk, K.; Bernath, P.F.; Colin, R. Infrared Emission Spectra of BeH_2 and BeD_2. *J. Chem. Phys.* **2003**, *118*, 3622-3627.

(39) Koput, J.; Peterson, K.A. Ab Initio Prediction of the Potential Energy Surface and Vibration-Rotation Energy Levels of BeH_2. *J. Chem. Phys.* **2006**, *125*, 044306.

(40) Li, H.; Le Roy, R.J. An Accurate Ab Initio Potential Energy Surface and Calculated Spectroscopic Constants for BeH_2, BeD_2, and BeHD. *J. Chem. Phys.* **2006**, *125*, 044307.

(41) Poshusta, R.D.; Klint, D.W.; Liberles, A. Ab Initio Potential Surfaces of BeH_2^+. *J. Chem. Phys.* **1971**, *55*, 252-262.

(42) Hinze, J.; Friedrich, O.; Sundermann, A. A Study of Some Unusual Hydrides: BeH_2, BeH_6^+ and SH_6. *Mol. Phys.* **1999**, *96*, 711-718.

(43) Page, A.J.; Wilson, D.J.D.; von Nagy-Felsobuki, E.I. Trends in MH_2^{n+} Ion-Quadrupole Complexes (M = Li, Be, Na, Mg, K, Ca; n = 1, 2) using Ab Initio Methods. *Phys. Chem. Chem. Phys.* **2010**, *12*, 13788-13797.

(44) Knowles, P.J.; Hampel, C.; Werner, H.-J. Coupled Cluster Theory for High Spin, Open Shell Reference Wave Functions. *J. Chem. Phys.* **1993**, *99*, 5219-5227.

(45) Alexander, M.H. Theoretical Investigation of Weakly-Bound Complexes of $O(^3P)$ with H_2. *J. Chem. Phys.* **1998**, *108*, 4467-4477.

(46) Boys, S.F.; Bernardi, F. The Calculation of Small Molecular Interactions by the Differences of Separate Total Energies. Some Procedures with Reduced Errors. *Mol. Phys.* **1970**, *19*, 553-566.

(47) Dunning, Jr., T.H. Gaussian Basis Sets for Use in Correlated Molecular Calculations. I. The Atoms Boron through Neon and Hydrogen. *J. Chem. Phys.* **1989**, *90*, 1007-1023.

(48) Cybulski, S.M.; Toczyłowski, R.R. Ground State Potential Energy Curves for He_2, Ne_2, Ar_2, He–Ne, He–Ar, and Ne–Ar: A Coupled-Cluster Study. *J. Chem. Phys.* **1999**, *111*, 10520-10528.

(49) Prascher, B.; Woon, D.E.; Peterson, K.A.; Dunning, Jr., T.H.; Wilson, A.K. Gaussian Basis Sets for Use in Correlated Molecular Calculations. VII. Valence, Core-Valence, and Scalar Relativistic Basis Sets for Li, Be, Na, and Mg. *Theor. Chem. Acc.* **2011**, *128*, 69-82.

(50) Cencek, W.; Szalewicz, K. Ultra-High Accuracy Calculations for Hydrogen Molecule and Helium Dimer. *Int. J. Quantum Chem.* **2008**, *108*, 2191-2198, and private communication.

(51) MOLPRO, version 2010.1, A Package of Ab Initio Programs written by Werner, H.-J.; Knowles, P.J.; Knizia, G.; Manby, F.R.; Schütz M.; and others, `http://www.molpro.net`.

(52) Ho, T.S.; Rabitz, H. A General Method for Constructing Multidimensional Molecular Potential Energy Surfaces from Ab Initio Calculations. *J. Chem. Phys.* **1996**, *104*, 2584-2597.

(53) Lawson, D.B.; Harrison, J.F. Distance Dependence and Spatial Distribution of the Molecular Quadrupole Moments of H_2, N_2, O_2, and F_2. *J. Phys. Chem. A* **1997**, *101*, 4781-4792.

(54) Ralchenko, Yu.; Kramida, A.E.; Reader, J. and NIST ASD Team, *NIST Atomic Spectra Database* (ver. 4.0.1) (National Institute of Standards and Technology, 2010), `http://physics.nist.gov/asd`.

(55) Raimondi, M.; Gerratt, J. Spin-Coupled VB Description of the Potential Energy Surfaces for the Reaction $Be^+ + H_2 \rightarrow BeH^+ + H$. *J. Chem. Phys.* **1983**, *79*, 4339-4345.

(56) Delgado-Barrio, G.; Beswick, J.A. In *Structure and Dynamics of Non-Rigid Molecular Systems*, Smeyers, Y.G.; Ed.; Kluwer: Dordrecht, 1994, pp.203-247.

(57) Reid, B.P.; Janda, K.C.; Halberstadt, N. Vibrational and Rotational Wave Functions for the

Triatomic van der Waals Molecules Helium Dichloride, Neon Dichloride, and Argon Dichloride. *J. Phys. Chem.* **1988**, *92*, 587-593.

(58) Reed, A.E.; Weinhold, F. Natural Localized Molecular Orbitals. *J. Chem. Phys.* **1985**, *83*, 1736-1740.

(59) Grinev, T.A.; Buchachenko, A.A.; Krems, R.V. Separation of ortho- and para-Hydrogen in Van der Waals Complex Formation. *ChemPhysChem* **2007**, *8*, 815-818.

Be^+-H_2	
D_0, cm^{-1}	3168
R_e, Å	1.776
r_e, Å	0.768
D_0, cm^{-1}	2667.68
$\bar{R}$, Å	1.828
$\bar{r}$, Å	0.763
A, cm^{-1}	66.198(1)
B, cm^{-1}	3.0517(5)
C, cm^{-1}	2.8542(5)
$\overline{B}$, cm^{-1}	2.95295
$\Delta\nu_{HH}$, cm^{-1}	-323

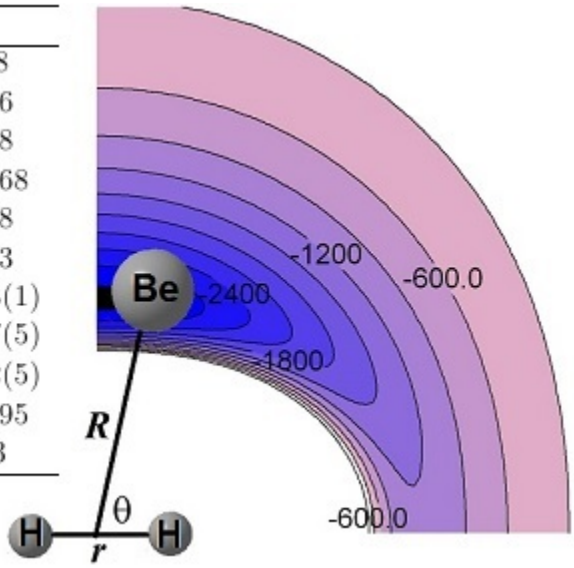

Author/s:
Artiukhin, DG; Klos, J; Bieske, EJ; Buchachenko, AA

Title:
Interaction of the Beryllium Cation with Molecular Hydrogen and Deuterium

Date:
2014-08-21

Citation:
Artiukhin, D. G., Klos, J., Bieske, E. J. & Buchachenko, A. A. (2014). Interaction of the Beryllium Cation with Molecular Hydrogen and Deuterium. JOURNAL OF PHYSICAL CHEMISTRY A, 118 (33), pp.6711-6720. https://doi.org/10.1021/jp504363d.

Persistent Link:
http://hdl.handle.net/11343/52032

File Description:
Accepted version